An Acad Bras Cienc (2022) 94(Suppl. 2): e20210391 DOI 10.1590/0001-3765202220210391
Anais da Academia Brasileira de Ciências | *Annals of the Brazilian Academy of Sciences*
Printed ISSN 0001-3765 I Online ISSN 1678-2690
www.scielo.br/aabc | www.fb.com/aabcjournal

GEOSCIENCES

The 2019 northeast Brazil oil spill: scenarios

PAULO NOBRE, ANGELO T. LEMOS, EMANUEL GIAROLLA, ROSIO CAMAYO, LAERCIO NAMIKAWA, MILTON KAMPEL, NATÁLIA RUDORFF, DIEGO X. BEZERRA, JOÃO LORENZZETTI, JORGE GOMES, MANOEL B. DA SILVA JR, CARLA P.M. LAGE, RAFAEL L. PAES, CARLOS BEISL, MÁRCIO M. LOBÃO, PEDRO A. BIGNELLI, NAJLA DE MOURA, WOUGRAN S. GALVÃO & PAULO S. POLITO

Abstract: During the last quarter of 2019, the beaches, mangroves, and estuaries of Northeast Brazil received an unprecedented volume of crude oil from the sea, which became the worst environmental disaster ever to reach the Brazilian coast. The oil, having reached the shores completely unnoticed, left both society and government agents completely clueless on (i) where the oil was coming from; (ii) how much oil was still in the ocean to reach the shorelines; and (iii) which beaches were going to be affected next! By exploring remote sensing data and ocean numerical modeling, along with oil dispersion chemistry on sea water, this study investigates the possible origin and path of the spill and whether it could have been detected from space. The oil dispersion modeling simulations performed for this investigation revealed a possible region and timing of the oil spill, also indicating the likelihood of it being advected toward the shoreline under the ocean surface.

Key words: Northeast Brazil, scenarios, 2019 oil spill, satellite imagery, ocean modeling.

INTRODUCTION

The appearance of small tar balls and oil slicks along the sands of Brazilian beaches is a recurrent phenomenon to which beach goers have grown accustomed. Yet, the large blobs of oil that reached Brazilian shores between August and December 2019 opened a new chapter in the history of petroleum pollution on the Brazilian shore. It represents the worst oil spill disaster not only in Brazilian history, but also in any tropical coastal region worldwide (Sissini et al. 2020). The amount and geographical extent of the shoreline affected by successive deposition of crude oil were unprecedented; however, it was not only the extension and unprecedented amounts of oil reaching Brazil's shoreline that were extraordinary. Both its origin and volume were unknown at the time. Eventually, and under the provisions of the National Contingency Plan - PNC, the Federal Government activated the Monitoring and Evaluation Group - GAA, jointly coordinated by the Brazilian Navy, the Brazilian Institute of Environment and Renewable Natural Resources - IBAMA, and the National Petroleum Agency - ANP. In addition to the coordination of actions combating the overwhelming amount of oil reaching Brazilian shores each day, the GAA created a scientific coordination body composed of seven working groups (WGs) that collaborated with scientists working voluntarily from all over the country. The objective of the scientific WGs was to advise and promote remediation actions by the GAA rooted in the best scientific knowledge available at the time. WG 1, which dealt with Monitoring and

Modeling, soon amassed some 50 atmospheric, ocean, and oil dispersion modelers, as well as satellite experts from several institutions, both public and private, from across the country. The other six WGs dealt with Biotic and Abiotic Factors, Socioeconomic Impacts, Protected Areas, Beaches, Mangroves, and Reefs. The WGs worked independently, having presented their recommendations for further actions and research at a workshop hosted by the Brazilian Navy at the Naval Warfare School in Rio de Janeiro, on 7–8 December 2019.

In the sequence, the National Council of Scientific and Technological Development - CNPq called for proposals in 2020 to study the several environmental and socioeconomic implications of the 2019 oil spill. From the over 120 proposals submitted, 11 were funded. These funded research projects cover many aspects of the 2019 oil spill disaster, ranging from mangrove restoration, to social impacts, to detection and modeling aspects of the oil spill, which is the topic of this article.

The oil reaches Brazil's shoreline

One of the most severe environmental disasters on the Brazilian coast was noticed with the first appearance of oil slicks on August 30, 2019, on the beaches of Paraiba's southern region (Figure 1a and 1b). During September, oil slicks appeared to the north and south of the first sightings, arriving at the beaches of Pernambuco and Rio Grande do Norte. To mitigate the numerous and serious environmental and socio-economic effects that could be caused by oil contamination, citizens quickly volunteered to participate in beach cleaning and response actions of the GAA. By the end of September, oil slicks had already

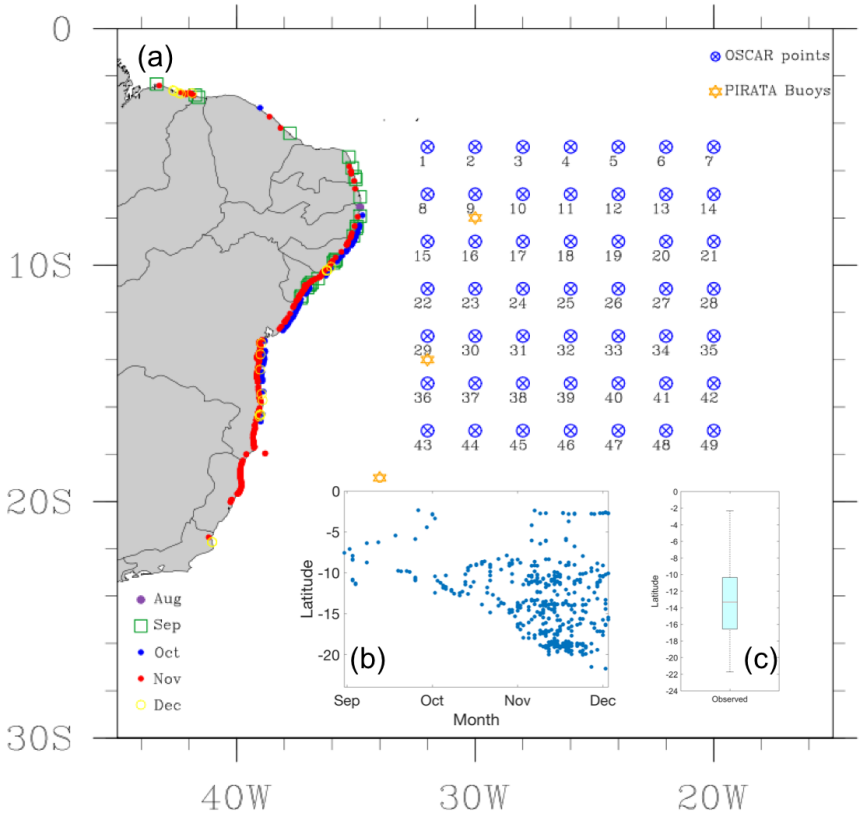

Figure 1. (a) Reported observations of oil slicks along the Brazilian coast during the period of August 30 to December 2, 2019 (Data source: IBAMA). Also shown are the 49 oil spill sites (blue circle-x marker) that were used in the numerical simulations with the OSCAR model. PIRATA buoy positions (orange star marker). (b) Latitudinal – temporal distribution of observed oil. (c) Box-plot of all observations of oil stains as a function of latitude. From bottom to top, the box-plot represents the minimum value, the first quartile, the median, the third quartile, and the maximum value.

been observed on several beaches between the Sergipe and Maranhão coasts. Between October and December, 11 Brazilian states were affected by the environmental tragedy, with oil slicks observed on many beaches along the coast of the Northeast Region, as well as in several locations on the coast of Espírito Santo and north of the Rio de Janeiro states. The largest amount of oil slicks and residue (75%) were sighted south of 10°S, with 50% of the sightings around 13°S (Figure 1c).

Most of the results of chemical analyses of collected oil samples indicated that the same heavy and slightly altered oil had reached the Brazilian coast between the states of Maranhão and Rio de Janeiro. According to oil biomarker analyses performed in the official forensic laboratory of the Brazilian Maritime Authority (Brazil's Navy - IEAPM), the spilled oil has geochemical characteristics very similar to some Venezuelan crudes (Lobão et al. 2010, López & Mónaco 2017, Oliveira et al. 2020) instead of a Brazilian sourced oil. As the source of the oil was not known, its characteristics had to be determined from samples collected in the beaches. Such samples were subjected to weathering effects that can cause considerable changes in physical properties and chemical composition (Peters et al. 2005, Wang et al. 2006, Stout & Wang 2007, Lobão et al. 2010). These heavy oil samples, which had lost volatile compounds (as evidenced by depletion of n-alkanes below n-C_{13}), prevented determination of its original density (API gravity) or viscosity. Some tests carried out by IEAPM determined that the density of the spilled oil was slightly higher than that of seawater (M. Lobão personal communication). No viscosity tests were performed by IEAPM due to the characteristics and contamination of the collected samples. As oil density changes with weathering, heavy oil spills may, under turbulent sea conditions, submerge in the water column. In the absence of turbulence typically associated with rough sea conditions, this oil can refloat later or permanently sink (American Petroleum Institute 2016). Such behavior explains the problems faced by the response teams in detecting the oil while it was at sea, as it traveled below the sea surface and resurfaced only when the sea conditions became milder, typical of overwashed oils.

As part of the incident response, oil samples from other sources, even including garbage (plastic and other materials), were collected on beaches in the affected regions and in other areas not affected by the incident. These samples were also analyzed by IEAPM. These oily samples, represented by very weathered tar balls, indicated that older oil spills had hit not only the same region, but also other areas not affected by the serious spill. Most likely, such smaller spills were detected only due to concern from the local population, and these incidents can be categorized as smaller, chronic spills, similar to those observed in other regions of the world (M. Lobão personal communication).

State of the ocean and atmosphere

During the occurrence of an oil spill, meteo-oceanographic conditions play an important role in the evolution of oil transport and physico-chemical processes, being very useful for emergency response operations. Ocean circulation is a key factor in determining the drift of spilled marine pollutants (Prasad et. al. 2019), mainly because oil trajectories tend to follow the directions of currents (Tessarolo 2017, Barreto 2019). In the present study, the OSCAR oil model was forced by daily current data from the global high-resolution PSY4V3R1 system, which was provided by the Mercator ocean monitoring and forecasting system in the framework of Copernicus Marine Environment Monitoring Service (CMEMS) (Lellouche et al. 2018).

The highest occurrence of coastal oil slick sightings was at 13°S. At this latitude in August 2019, the vertical-longitudinal structure of the potential water temperature distribution (data not shown) indicates warmer water above 100 meters deep relative to the climatological mean in the area between the Brazilian coast and 32°W. This warmer water persisted to the west of 32°W during the months of September and October 2019, extending further east in November 2019. The 20°C isotherm was observed between depths of approximately 140 and 200 meters from August to November 2019.

MATERIALS AND METHODS

The origin: backward parcel trajectories

One of the first attempts to identify the position and time of the origin of the oil spill that reached the northeast Brazil coast used a Lagrangian model to backtrack the water parcels that transported the oil to the Brazilian shoreline. In such Lagrangian methodologies, after the definition of an ocean current field, a certain number of tracers are released at any position of the domain, and the path of each one is simulated individually. Such tracers can also be deployed at any time, not just at the simulation beginning. The objective here was to perform a simulation, backward in time, with a certain number of tracers released at positions and dates similar to those where the presence of oil was first reported on the Brazilian coastline. Therefore, this backward Lagrangian simulation was used to give first guesses of positions and dates from where the oil spill dispersion model should start its integrations, forward in time.

The Lagrangian model used for this simulation is OceanParcels (Lange & van Sebille 2017, Delandmeter & van Sebille 2019), with hourly surface ocean currents from Mercator datasets (Drevillon et al. 2018, among others) applied as the basic ocean flow field. A table from IBAMA provided the positions and dates of the first detection of oil on the coast, so the tracers were deployed at those positions and dates. The model ran backwards with a 6-h time step from November 2019 to July of the same year. Figure 2 presents the main conclusions of this experiment.

To illustrate the process, Figure 2a,b shows a representation of the tracers' positions on September 16 and on July 16, respectively. The purpose, as mentioned before, was to determine an area of convergence of those tracers to be used as a reference for experiments executed by the oil spill dispersion model (supposing that such concentration areas would represent possible sources of oil spill). Figure 2c can help with this purpose, showing a histogram of the tracers' concentrations encompassing the entire simulation. A region of concentration between approximately 12°S–6°S, 25°W–35°W was identified (Figure 2c), and Figure 2b suggests that the peak of this concentration might have occurred around July. This result was used as a basis for the oil spill simulations discussed in the next section.

A second independent set of backward Lagrangian simulations was performed with the same software but with different ocean currents. In this set, we used the ocean currents provided by the MULTIOBS_GLO_PHI_NRT_015_003 product distributed by the Copernicus Marine Environment Monitoring Service (CMEMS) (Rio et al. 2014). The same processing was applied using the velocities at 15 m of depth from the same input dataset. Results from this simulation (not shown) are consistent with the ones for the surface. The smaller velocities at 15 m decreased the westward zonal reach of the trajectories, yet the pathways were similar in the sense that they seem to follow the SEC and then spend some time slowly circulating.

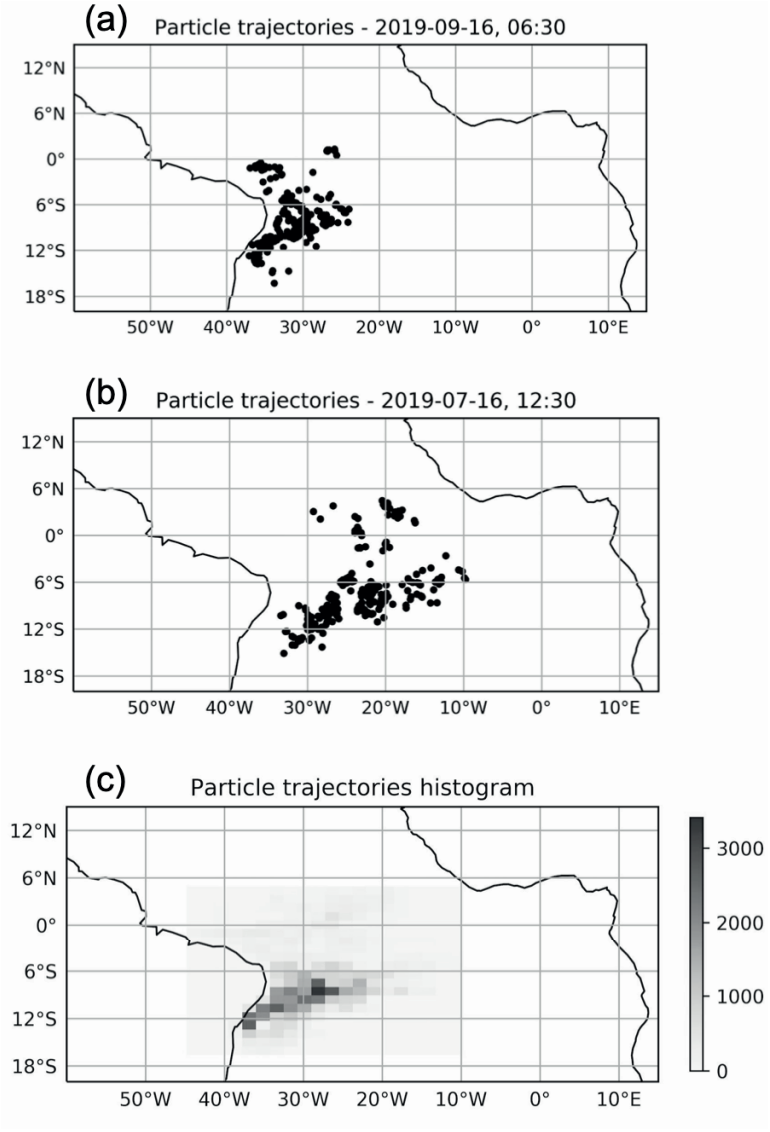

Figure 2. Snapshots, from a backward OceanParcels simulation (see text), showing the particle locations on days (a) September 16 and (b) July 16, 2019, and (c) a histogram representing the concentration of particles during the entire simulation period.

The origin: forward oil spill dispersion

One of the tools available to reconcile the paths between oil exploration on the seafloor and environmental preservation is oil spill modeling. A large number of such models are currently used by the scientific community, ranging from parcel trajectory determination or particle monitoring to three-dimensional models of oil trajectories that include response actions and biological processes in their simulations, among others (Reed et al. 1999).

In this study, we use the OSCAR (Oil Spill Contingency and Response) model in deterministic mode (Reed et al. 1999) to investigate the distribution of coastline positions affected by oil in individual oil spill experiments. The OSCAR model considers weathering processes such as advection, spreading, evaporation, natural dispersion, emulsification, dissolution, biodegradation, and sedimentation. The evaporation, dissolution, and degradation processes are directly related to the mass of each oil component and are dynamically calculated at each time step. The

spreading, entrainment, and vertical mixing processes are more directly related to the oil density and viscosity. Waves in the model are simulated based on 10-meter wind speeds and the JONSWAP spectrum (Hasselmann et al. 1973).

The study is focused on processes related to oil weathering at sea (evaporation, surface oil, water column, biodegradation, sedimentation, and presence on the coast) and the distribution of ashore oil along the Brazilian coast within the period of simulation in each experiment. The simulation results are contrasted with in situ observations provided by IBAMA through December 2, 2019. The uncertainty regarding the date of the alleged leak does not allow us to infer the exact day of the spill; however, considering the date of the first sighting and the meteo-oceanographic conditions around the northeast coast of Brazil (up to 700 km offshore), it is possible to assume that the spill event occurred between the months of June and August.

A total of 49 simulation experiments were carried out with the initial date July 29 until December 2, 2019 (127 days), with the oil spill locations between the latitudes of 5°S and 17°S and the longitudes of 32°W and 20°W, as depicted in Figure 1. The hydrodynamic (daily zonal and meridional velocity components) and atmospheric (zonal and meridional wind components at 10 m) forcing data are from Mercator and ERA5, respectively, both with 10 km spatial resolution. The data of the annual average water column temperature and salinity up to 100 meters are from in situ measurements by the PIRATA moored buoy array (Bourlès et al. 2008, 2019) at 8°S, 30°W as depicted in Figure 1.

According to oil biomarker analyses performed by IEAPM, the spilled oil has geochemical characteristics very similar to some Venezuelan crudes (Lobão et al. 2010, López & Mónaco 2017, Oliveira et al. 2020). Considering the available information and the characteristics of the oil, the most severe oil pollution ever seen on the Brazilian coast was probably caused by a spill of heavy or extra-heavy crude oil or even a heavy fuel oil (HFO) sourced in the Venezuelan basin. Therefore, the simulations used a Bunker oil of °API 14 and viscosity of 28000 cP, as being representative oil of the heavy and high viscosity oil group. The chemical composition of the oil according to the model database can be seen in Table I.

For the simulations, 100,000 tons of oil spilled into the sea over 2 days was chosen based on the hypothesis that the leak came from an oil tanker. This value is consistent with the maximum transport capacity of some types of oil tankers present in the commercial fleet, such as Aframax and Suezmax (Northern Gateway Pipelines Inc. 2010). The other characteristics of the simulations can be seen in Table II.

Figure 3 shows the latitudinal distribution of the ashore oil for each experiment (as box plots) compared with the IBAMA sighting data through December 2, 2019. One of the main aspects observed is that individually, few of the experimental outcomes were similar to what was observed, mainly concerning the maximum and minimum limits of latitude. Thus, the possibility that a single fixed source of the oil spill caused the observed latitudinal spreading is low.

A few experiments have 25% and 75% percentile limits (lower and upper levels of the boxes, respectively) similar to or within the limits of the percentiles of the observed scenario. Thus, the possibility of a mobile spill source, rather than a fixed source as modeled by the numerical oil spill experiments, was also considered. In this approach, three criteria were considered for combining the boxplots: (i) some of the percentiles (25% or 75%) of at least one of the experiments must be within the limits of the observed percentiles, (ii) the experiments must be adjacent to each other, to determine

Table I. Chemical composition of the oil used in the experiments.

Percentage (%)	Oil components
0.000000	C1-C4 gasses (dissolved in oil)
0.000000	C5-saturates (n-/iso-/cyclo)
0.000000	C6-saturates (n-/iso-/cyclo)
0.000000	Benzene
0.000000	C7-saturates (n-/iso-/cyclo)
0.000000	C1-Benzene (Toluene) et. B
0.000000	C8-saturates (n-/iso-/cyclo)
0.132727	C2-Benzene (xylenes; using O-xylene)
0.540886	C9-saturates (n-/iso-/cyclo)
0.720851	C3-Benzene
1.880224	C10-saturates (n-/iso-/cyclo)
0.064835	C4 and C4 Benzenes
1.644173	C11-C12 (total sat + aro)
0.002616	Phenols (C0-C4 alkylated)
0.088681	Naphthalenes 1 (C0-C1-alkylated)
1.775817	C13-C14 (total sat + aro)
0.162399	Naphthalenes 2 (C2-C3-alkylated)
2.261291	C15-C16 (total sat + aro)
0.097961	PAH 1 (Medium soluble polyaromatic hydrocarbons (3 rings-non-alkylated; <4 rings)
1.100772	C17-C18 (total sat + aro)
0.845334	C19-C20 (total sat + aro)
0.018919	Unresolved Chromatographic Materials (UCM: C10 to C36)
1.575727	C21-C25 (total sat + aro)
0.014825	PAH 2 (Low soluble polyaromatic hydrocarbons (3 rings-alkylated; 4-5+ rings)
87.071963	C25+ (total)

a continuous route with a greater probability of occurrence and, (iii) there must be a vertical expansion of the combined box in some of the percentile limits between the experiments. Table III shows how the boxplots of various experiments were combined, and Figure 4 shows the results of the merged boxplots compared with the ashore observed oil (depicted by the thick black line alongshore in Figure 5a). Experiment 24 was added to form a highlighted polygon (shown in Figure 1).

The boxplot combinations revealed the combinations of experiments whose results mirrored the distribution of ashore oil considering a mobile spill source, such as an in-transit oil tanker. In addition to the possible experiments, another objective of combining the boxplots was to establish, based on the meteo-oceanographic conditions of the region at the

Table II. Model parameters.

Number of liquid/solid particles	2000
X direction resolution [m]	2980
Y direction resolution [m]	2900
Z direction	10
Maximum concentration grid depth [m]	100
Time step [seconds]	1200

time, the characteristics of the oil and, based on the initial conditions of the experiments, the most likely region in which the spill had occurred. Experiments 22 and 23 were present in six combinations, and together with experiment 29 (combinations 2 and 4) they showed that a mobile spill source in this region or nearby could have caused the ashore oil in the observed proportions.

To analyze in more detail how the oil weathering process might have occurred in this region, experiment 22 (marked by the red x in Figure 5a) was chosen to represent the time series of the oil mass balance (Figure 6). In this experiment, it was possible to observe that at the end of the simulation, almost 60% of the spilled oil underwent biodegradation, while 18% reached the coast, 10% precipitated on the seabed, and 15% evaporated. In this experiment, the oil reached the coast 13 days after the start of the simulation, reaching a maximum quantity of almost 20,000 tons. Table IV shows the maximum amount of oil and minimum time of arrival on the coast for each of the 49 experiments shown in Figure 5a, with emphasis on the experiments that were combined in the boxplot analysis (light gray). The averages of the minimum time of arrival at the coast and the maximum amount of oil from these experiments were 30.6 days and 6,951 tons, respectively.

In the first 10 days of simulation of experiment 22, the oil amount on the surface decreased from 94% to 42%, while the amount present in the water column increased from 2% to 42% (Figure 6). This result suggests that the weathering of the oil provided a fast submersion, rapidly reducing the amount of oil present on the surface. This phenomenon might have contributed to the low occurrence of oil observation on the surface through in situ and remote sensing investigations, as detailed in the next section. To analyze the presence of oil in the water column, a vertical concentration profile was derived for August 8 in experiment 22 (11 days after the start of the simulation) through a zonal section, as shown in Figure 5b,c.

Subsurface oil concentration was present to approximately 60 meters deep 11 days after the start of the simulation, with concentration cores between 10 and 25 meters. It is assumed based on the chemical characteristics of this heavy and viscous oil that it spread to the subsurface and

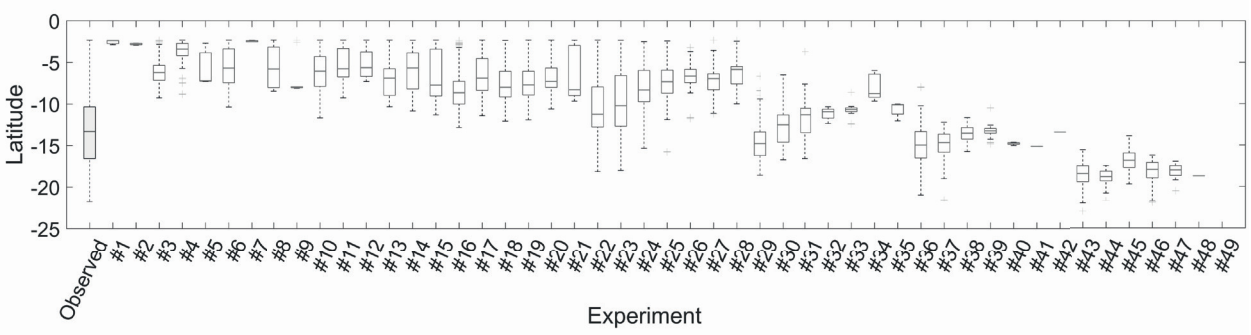

Figure 3. Results of the boxplot experiments. The boxplot of the observed scenario of ashore oil is highlighted in gray.

Table III. Combined boxplot experiments.

Combination	Experiments
1	[#22 e #23]
2	[#22 e #29]
3	[#22 e #30]
4	[#23 e #29]
5	[#23 e #30]
6	[#23 e #31]
7	[#29 e #30]
8	[#29 e #36]
9	[#30 e #31]
10	[#30 e #37]
11	[#31 e #38]

reached the seabed of the Brazilian continental shelf before reaching the beaches. It is possible, therefore, that even on a smaller spatial scale, resuspension processes could bring up small amounts of this oil back to the beaches by wave action and later storm events.

Earth observation (EO) data used as an attempt to detect mineral oil slicks on their way to the shore

When the first packages of mineral oil arrived at the northeastern Brazilian coast (end of August to beginning of September 2019), the first efforts to detect and track a surface oil slick used synthetic-aperture radar (SAR) imagery (Sentinel-1 A/B) complemented by auxiliary high-medium resolution optical imagery (Sentinel 2 A/B, CBERS-4). This effort was performed in a collaboration between INPE and NOAA, covering the entire northern and northeastern Brazilian coast (8N-18S), using images acquired from August to October 2019. NOAA Office of Satellite and Product Operations (OSPO) reported no detectable surface mineral oil slicks throughout the region and period analyzed (NOAA 2019).

For the detection of oil slicks in Sentinel-1 images, an additional effort was carried out in which around 100 images were analyzed using the unsupervised semivariogram textural classifier (USTC) methodology. This method

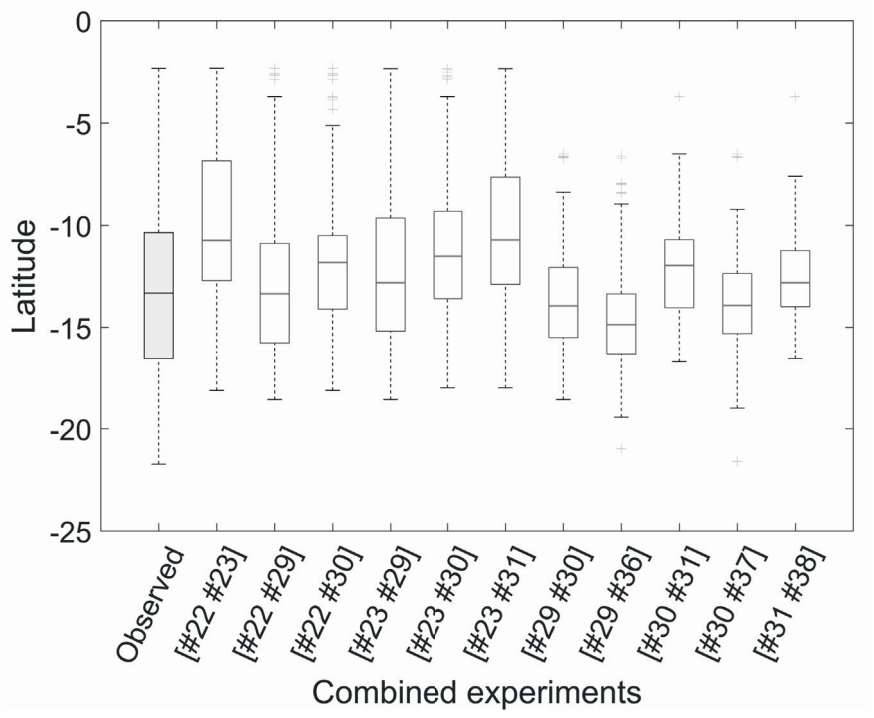

Figure 4. Results of the combined boxplot experiments. The boxplot of the observed scenario of ashore oil is highlighted in gray.

uses a semivariogram function as a textural descriptor based on considering pixel values in the context of their neighbors, and is efficient for the digital treatment of SAR images (Miranda et al. 1997). The USTC methodology can discriminate areas with distinct roughness on the sea surface, allowing the identification of oil stains and maintaining the spatial and radiometric accuracy of the feature (Miranda et al. 2004). Approximately 24 dark features found in Sentinel-1 images were analyzed (Figure 7). Of these, 23 were interpreted as oil slicks; however, their origins were not related to the oil slick event in question (Figure 8 a,d).

In parallel, several Brazilian researchers and remote sensing experts from universities and private companies made their own efforts to detect a surface oil spill with publicly available Earth observation (EO) imagery. Some suspected features shown in Figure 9 a,b were eventually reported by some researchers. For each of the reported suspected features, a thorough analysis was elaborated at INPE via the use of a suite of ocean remote sensing products including Sentinel-1 A/B SAR and high-medium optical imagery (Sentinel 2 A/B, CBERS-4) integrated with auxiliary meteo-oceanographic satellite products, including remote sensing reflectance (Rrs) and chlorophyll-*a* concentration (Chl-a) analyzes as well as sea surface temperature (SST) data derived from the MODIS-Aqua/Terra, VIIRS-SNPP/JPSS1, and OLCI-Sentinel 3 A/B

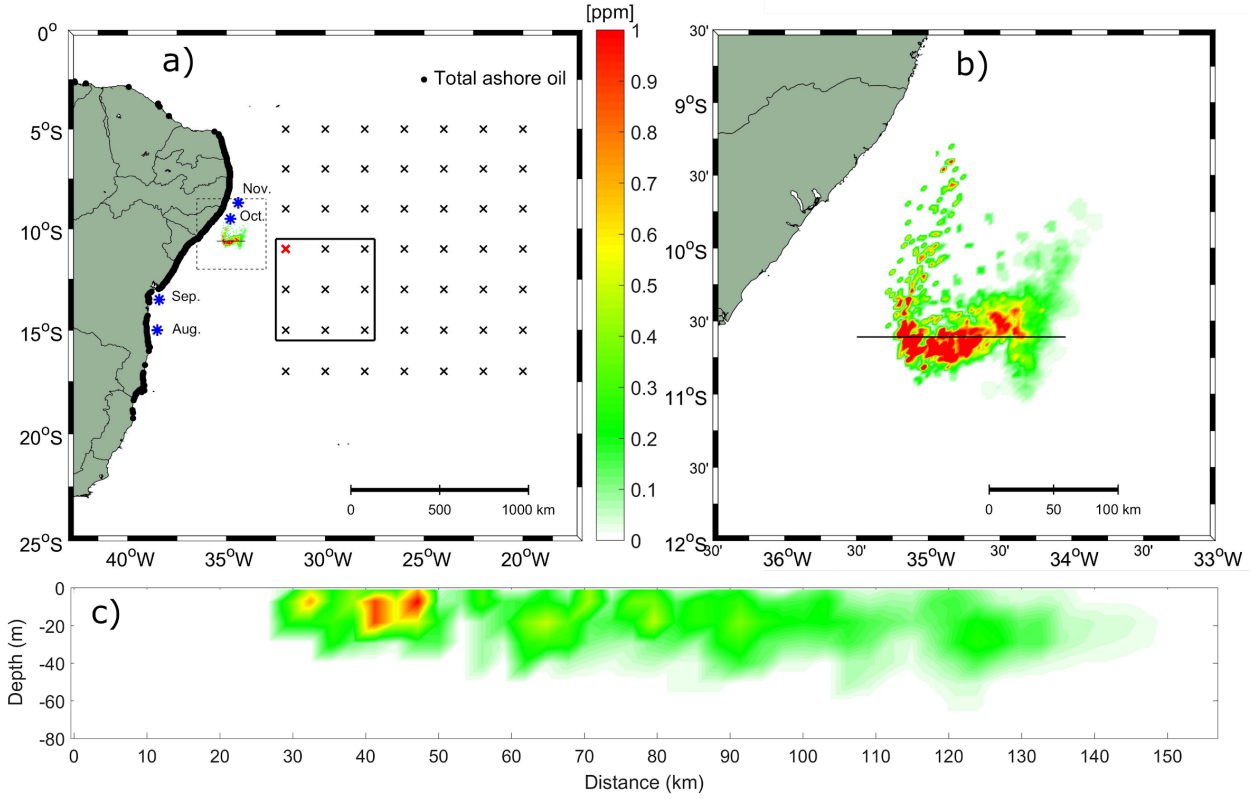

Figure 5. (a) Total ashore oil (black dots) from experiment 22 (red "x") after 127 days. The blue stars mark the monthly mean position of the South Equatorial Current Bifurcation from August to November provided by Mercator Ocean. The solid black polygon delimits the possible source area identified by the oil spill modeling. The dashed polygon delimits the integrated water column (up to 100 m) oil spreading at day 11 from experiment 22, highlighted in (b). (c) Oil concentrations in the water column on day 11 along the black line in (b).

sensors; geostationary brightness temperatures (BT) and precipitation products from the ABI/GOES-16 sensor; and surface ocean wind vectors from ASCAT/MetOP-A/B/C and Scatsat-1.

The analyses performed at INPE revealed that all suspected features were either related to meteo-oceanographic conditions, i.e., influence of different water masses (SST gradients and frontal zones), phytoplankton patches, local shelf geomorphology (e.g., Figure 9), or rain cell effects suppressing the sea surface roughness on the SAR imagery (e.g., Figure 8 b,c), or even to minor oil spill events from local ship traffic. None of the reported suspected features proved to be related to the major oil spill disaster that affected the entire Brazilian North, Northeast, and even parts of the Southeast coast from August to December 2019 (IBAMA 2019).

The analysis of the EO imagery provided by INPE's specialists and collaborators were in some cases supported by aerial observation using high-resolution sensors provided by IBAMA and in all cases supported by hydrodynamic and oil dispersion modeling efforts that indicated different regions and periods of probable occurrence of the disaster (as shown in the previous sections of this report).

Since the region of probable occurrence of the major oil spill was revealed by modeling experiments as being far from the coastline (> 400 km), no SAR imagery (neither freely distributed nor commercial) was available to detect and track a surface oil slick before the mineral oil packages likely submerged to subsurface depths, where SAR detection is not feasible.

Additional efforts were made to detect any offshore oil slick on the sea surface using moderate resolution optical imagery (MODIS, VIIRS, and OLCI), but due to the robust challenges regarding mineral oil detection using this type of data, i.e., absence of sea surface sun glint effects, spectral confusion with the ocean background, different spectral properties of oil types, cloud cover limitation, and coarse spatial resolution (Leifer et al. 2012, Fingas & Brown 2017), no suspected feature was detected.

High spatial resolution imagery was also used tentatively to identify the oil just before its arrival on the coast (Figure 10). Assuming that the largest patches were among the first to arrive, that they were on the surface or just below the water level, and that they were large enough to be detected in image pixel sizes from 5 up to 20 meters (one-pixel-size objects are considered noise because at least a 2-by-2-pixel-size mineral oil patch is the limit of detection), CBERS4 images acquired over the region along the coast between the states of Paraíba and Alagoas on August 29, 2019, (path 146, rows between 108 and 111) were used to detect the patches just before the first landings. The first sightings of mineral oil in the region were reported between Cabedelo (Paraíba

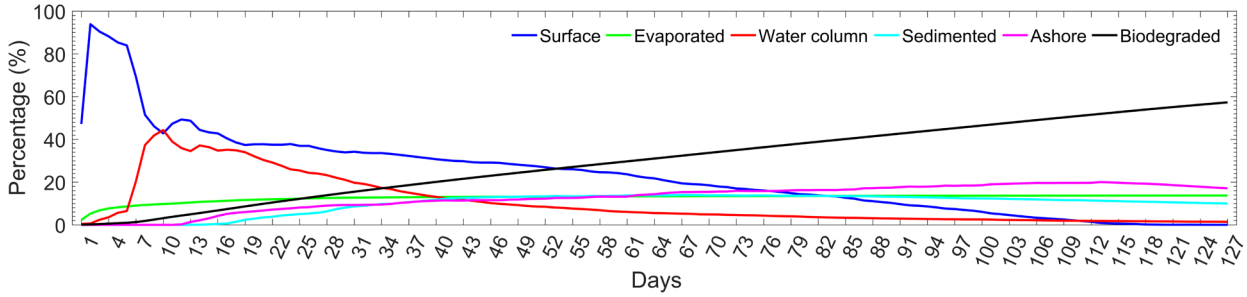

Figure 6. Temporal series of the oil mass balance from experiment 22.

state) and Tamandaré (Pernambuco state). Sea surface current maps from September 1, 2019, indicated that the current direction was from the Southeast to Northwest; thus, mineral oil patches could have been along the coast of Alagoas state during this period.

CBERS4 acquires images in the visible and near infrared range of the electromagnetic spectrum. These images can be analyzed in search of irregularities in the surface wave pattern and water reflectance. The hypothesis was that oil on the surface or just under it would affect wave patterns due to differences in the densities of sea water and oil. The reflectance of oil patches on the surface and under it at a certain depth are distinct from that of clean sea water. The PAN camera, with a spatial resolution of 10 meters in multispectral bands (green, red, and near-infrared) and 5 meters in a panchromatic band, reaches between 4 and

Table IV. Results of the maximum ashore oil and the minimum time of arrival. The experiments whose data were used in the combined boxplot analysis are highlighted in light gray.

Experiment	Maximum (tons)	Arrival day	Experiment	Maximum (tons)	Arrival day
1	33,43	18	**26**	845,86	42
2	0,0037	46	**27**	240,76	53
3	135,66	38	**28**	206,14	55
4	67,89	29	**29**	7088,03	27
5	220,08	20	**30**	4322,61	30
6	212,62	50	**31**	2926,42	36
7	27,87	83	**32**	2490,04	39
8	108,5	23	**33**	479,85	52
9	11,04	26	**34**	305	52
10	668,72	34	**35**	113,95	72
11	187,75	38	**36**	5902,46	33
12	220,08	26	**37**	3453,09	40
13	196,62	31	**38**	1687,23	47
14	261,96	54	**39**	619,47	57
15	5383,74	11	**40**	80,17	83
16	5472,34	21	**41**	31,51	90
17	1216,97	26	**42**	50,32	94
18	460,98	60	**43**	3179,88	47
19	301,62	51	**44**	590,21	59
20	187,92	64	**45**	2198,36	57
21	113,92	71	**46**	560,32	65
22	19998,3	13	**47**	1011,56	71
23	11304,3	21	**48**	40,29	92
24	5884,15	29	**49**	0	-
25	1774,61	35	Total (tons)		100.000

28 Km off the coast. While approximately 25% of the image data was obscured by clouds, a thorough visual analysis of the images did not detect any anomaly that could be related to the oil patches. The MUX camera, with a spatial resolution of 20 meters in multispectral bands (blue, green, red, and near-infrared) reaches a wider area than the PAN camera, between 62 to 75 Km off the coast. A thorough visual analysis of the MUX images revealed no spectral anomalies that could indicate the presence of mineral oil.

The currently available satellite remote sensing technology only allows the operational detection of mineral oil on the surface of the water (Fingas & Brown 2017). The failure to detect the oil that reached the Brazilian coast in the 2019 oil disaster suggests that the oil spill rapidly submerged to subsurface depths, where it was undetectable by both SAR and optical imagery, until it arrived near the coast, after which it appeared on beaches and in estuaries.

The interpretation of SAR images in oceanic regions requires the use of auxiliary data such as surface ocean wind vectors, sea surface temperature, sea surface chlorophyll-*a* concentration, and precipitation (for the identification of rain cells). An integrated, knowledge-driven analysis of such a collection of orbital data is particularly important for reducing uncertainty in the interpretation of oil-related features in surface oceanic regions.

SAR satellite coverage and vessel traffic ocean surveillance during the 2019 spill

Considering the large extent of the Brazilian coastal zone that was impacted by the 2019 oil spill as well as the large quantity of material involved, it is perhaps safe to exclude the possibility that the event was the result of natural causes, such as bottom exudations. Therefore, it is almost certain that it resulted from some man-made activity, e.g., an unexpected accident or operational mishap or a deliberate and criminal act of environmental terrorism. Whatever the cause or liable agent, it would be highly interesting to investigate the set of ships that were present in the region of interest (ROI) depicted in Figure 1 during the period of the spill, as they could possibly be the source of the oil. To this end, we analyzed a vessel traffic messaging data set from the Automatic Identification System (AIS) that includes cargo and oil ship positions during the period preceding the first sightings of oil slicks along the Brazilian shores.

SAR images are considered the most efficient satellite data for day and night monitoring of large ocean regions for oil spills and for ship detection. As soon as the first oil landings started, a search for oceanic SAR images of the ROI was initiated. The question was, of course, whether a suitable data set had been acquired for the ROI and period of interest in a timely fashion for analysis. As indicated below, the only SAR data freely available for analysis were from the Sentinel-1A and -1B satellites (S-1).

An analysis of a SAR data set acquired beginning one to two months before the first oil landings should have helped to monitor the oil spillage area on the sea surface as well as the displacement of any oil towards the coast while also pinpointing which detected vessel could have been the source of the oil. Considering that the first oil arrived on Brazilian beaches in late August 2019, we analyzed AIS and SAR S-1 data sets for the year 2019 with an emphasis on the period from late July through September. The objectives were to provide an account of the oil and cargo vessel traffic in the ROI and to assess how effectively the available Sentinel-1 SAR image data covered the ROI during that period.

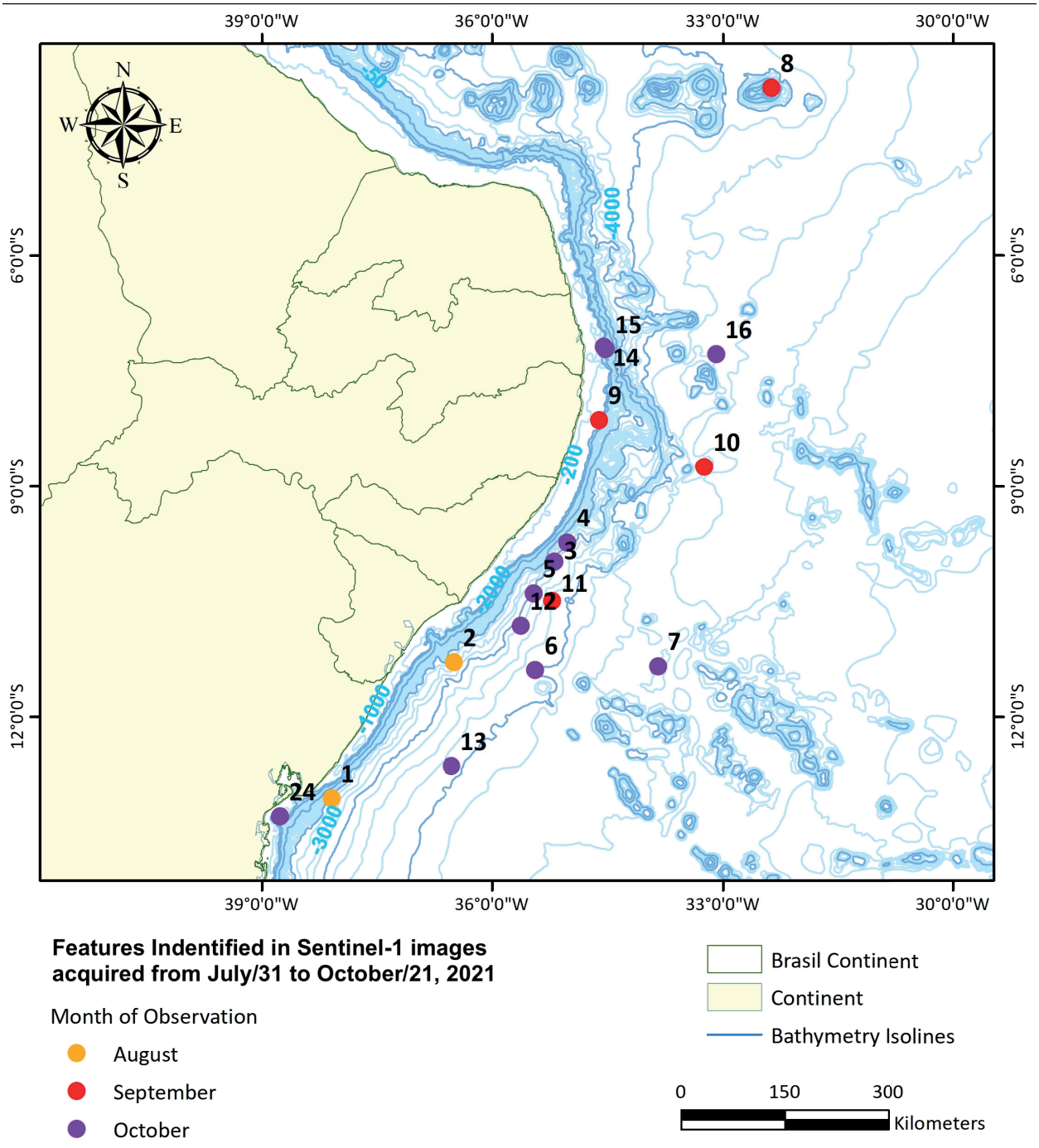

Figure 7. Dark features on the sea surface interpreted in 100 Sentinel-1 SAR images acquired from August to October, 2019.

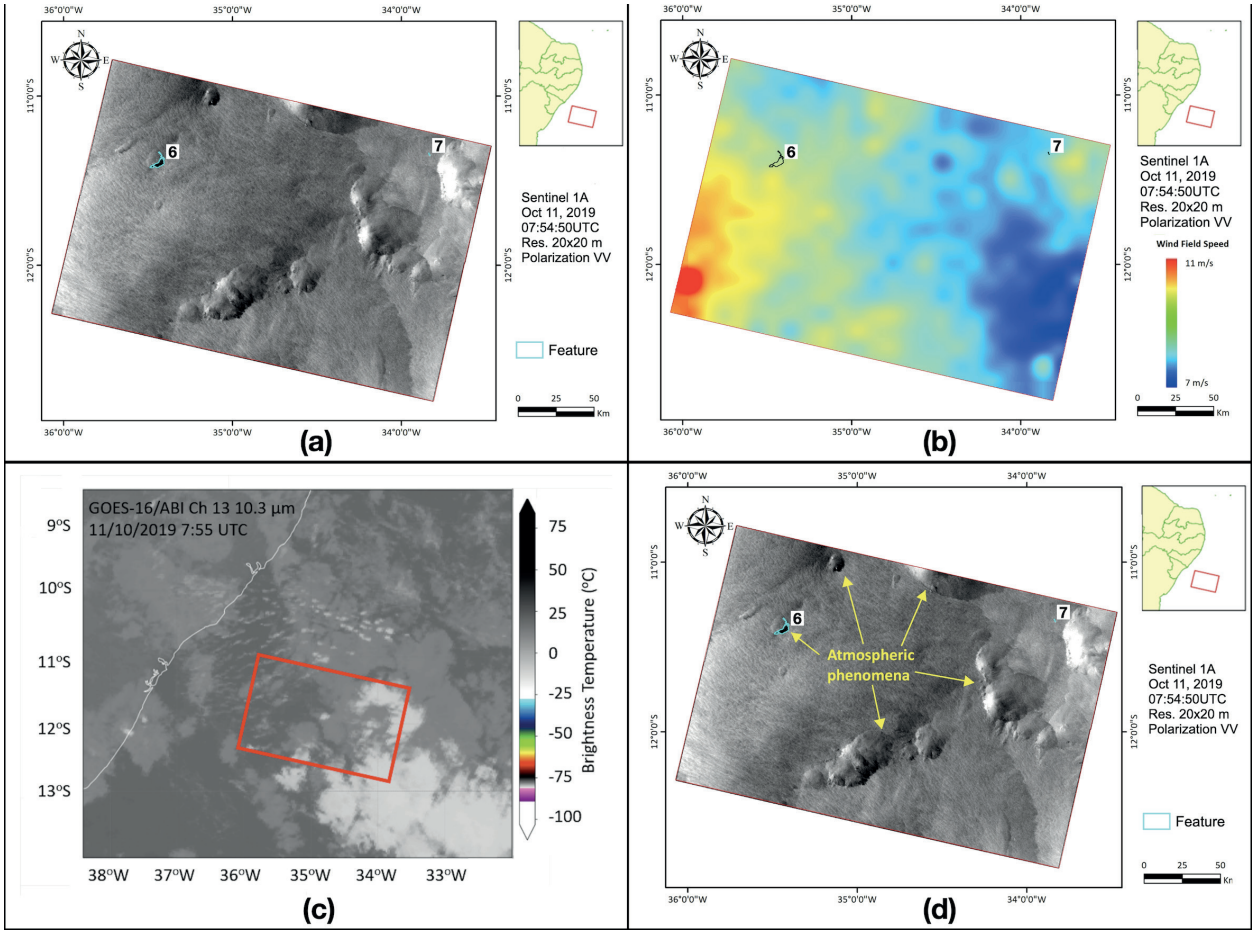

Figure 8. Set of images showing the interpretation of (a) a Sentinel-1 SAR image acquired on October 11, 2019, 07:54:50 UTC; (b) Sea surface wind speed derived from the Sentinel-1 SAR image; (c) GOES-16 image from October 16, 2019, 07:55: UTC; and (d) Interpretation of the various atmospheric phenomena in the Sentinel-1 SAR image, including rain cell effects (numbers 6 and 7 depict dark features shown in Figure 7).

The automatic identification system (AIS) and its data set

As noted in Annex 12 of the Maritime Safety Committee (MSC) of the International Maritime Organization (IMO) Resolution MSC.74(69) of 12 May 1998, the AIS was developed to "*improve the safety of navigation by assisting in the efficient navigation of ships, protection of the environment, and operation of the vessel traffic services (VTS).*" Furthermore, it should satisfy the following functional requirements: "*1) in a ship-to-ship mode for collision avoidance; 2) as a means for littoral states to obtain information about a ship and its cargo; and 3) Vessel Traffic Services tool, i.e.[,]ship-to-shore (shore management).*" In its satellite system mode, the AIS system provides the positions of ships based on global positioning system (GPS) and Global Navigation Satellite System (GLONASS) signals at nominal accuracies of approximately 35 m in non-differential mode and approximately 10 m in differential mode. It should also generate and output position solutions at least once every second.

It is to be noted, however, that some vessels either do not have an AIS transmitter or have a non-functional (i.e., non-transmitting) AIS transmitter, either intentionally or due to system malfunctions. Consequently, AIS data of ships in an oceanic area and for a specific time

period can be an under-representation of the true set of present vessels. The AIS data used in this paper were provided by the CISMAR/MB – Integrated Center for Maritime Security/Brazilian Navy.

By analyzing the trajectories of ships by combining the AIS transmissions with the same Ship Identification Code (instead of analyzing AIS transmissions alone), a clear view of the ship traffic during the period was obtained (Figure 11). From this analysis, 25 oil tankers were identified in routes intersecting the ROI. The two main offshore shipping lanes are again visible. The NW - SE lane, which links the Caribbean and South Africa and is the more likely site of the spill, lightly intercepts the upper right corner of the ROI. Therefore, it is tempting to hypothesize that one of the ships in that region could be the source of the oil; however, the oil spill drift model results presented in the previous section of this article suggest that this is a region of marginal probability. On the other hand, considering that both the circulation and the oil drift models are subject to some degree of uncertainty due to errors in model forcing fields and overly simplified parameterizations, we cannot exclude the possibility that the ROI is somewhat displaced to right such that there was a more probable contribution of ships in the NW-SE lane. The NE-SW shipping lane has a sizable overlap with the ROI, but considering the origin and destinations of this lane, it has a lower likelihood of being the origin of the oil. Of course, this conclusion lacks factual evidence. Furthermore, it should be noted that some ship trajectories with origins or destinations in the ports of Salvador, Recife, Fortaleza, and Rio de Janeiro were found crossing the ROI during the period of interest. Whether we should associate any of these ships with the spill is, however, difficult to support.

The Sentinel-1 SAR mission and data set

The Sentinel Program is the satellite component of the Global Monitoring for Environment and Security (GMES) program, the joint European Commission (EC) and the European Space Agency (ESA) Copernicus initiative. The Sentinel program includes 5 different satellite Earth observation (EO) missions, each focused on a different aspect of atmospheric, land, and oceanic monitoring and applications. Sentinel-1A and -1B (S-1A, S-1B) are synthetic-aperture radar (SAR) satellites designed for medium- to high-resolution applications that include high-resolution imaging of global landmasses, coastal zones, polar areas, sea ice, and shipping routes. The S-1A and S-1B image data used in this study was collected in IW (interferometric wide) mode at a spatial resolution of 10 m.

As a result of the environmental crisis of the oil spillage reaching the coast, a substantial effort was made by the European Space Agency (ESA) during the months of October and November of 2019 to increase the coverage of the SAR Sentinel-1 data in the region with the acquisition of Sentinel 1-B data. In total, 1353 S-1A and 368 S-1B images were acquired, with 1495 and 226 in descending and ascending orbit, respectively.

A review of the images acquired during the period of July to September, which is the most probable period of finding the oil spill or the responsible ship in the SAR images (Figure 12a, b, c), revealed that almost no SAR images were collected over the highest probability region (black rectangle). With the additional images acquired during October (Figure 12d) it was possible to cover the targeted area; however, these images were collected too late, during the least probable period for the detection of an oil spill or the responsible ship.

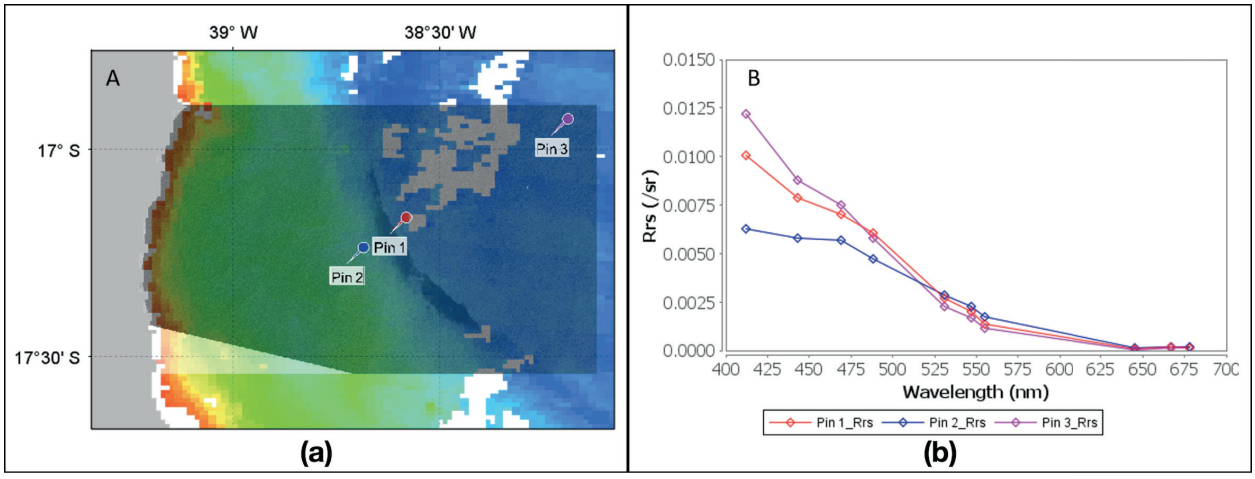

Figure 9. (a) Sea surface chlorophyll-*a* concentration derived from a MODIS-Terra image acquired on October 10, 2019, with the overlay of the Sentinel-1A SAR image obtained on the same day with a suspicious dark feature. **(b)** Remote sensing reflectance spectra at the collection points indicated in the MODIS chlorophyll image in **(a)**. The suspicious feature is observed in a frontal zone with a higher chlorophyll-*a* concentration at the shelf break. The spectral behavior on the suspicious feature does not indicate any spectral changes that can be associated with oil on the sea surface or subsurface. The dark feature was probably associated with the accumulation of biogenic surfactants at the frontal zone as well as sea bottom topography effects.

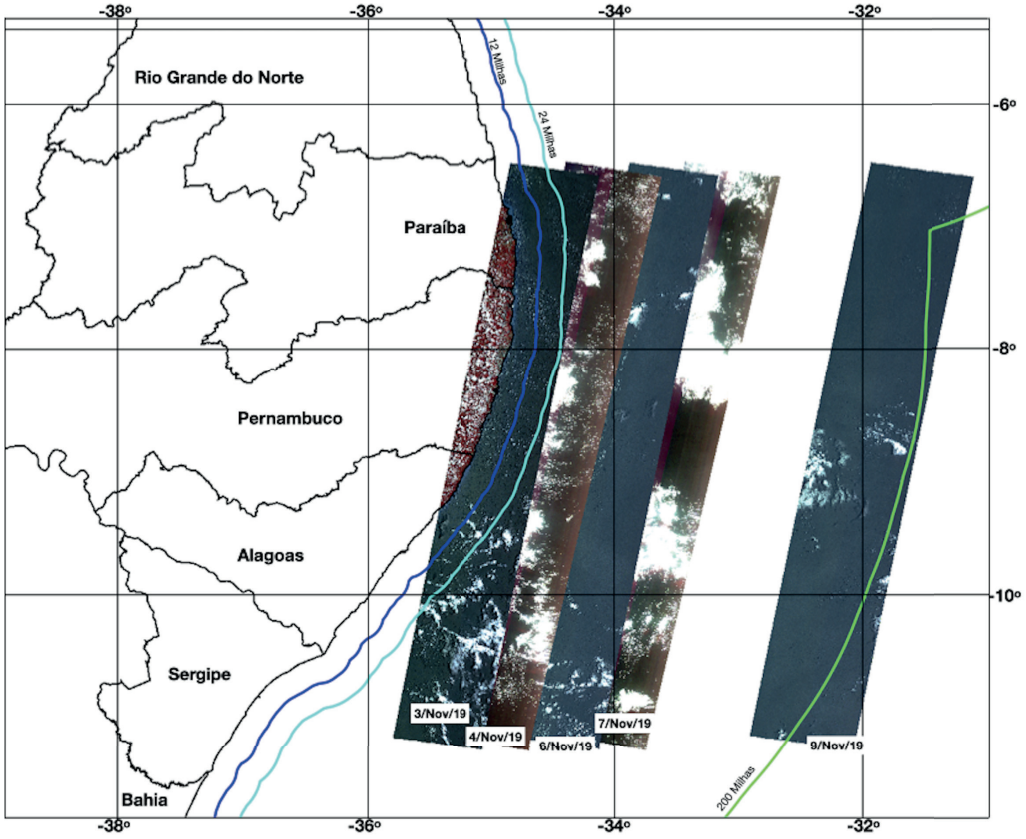

Figure 10. Paths/rows of CBERS-4 images acquired, by request, in November, 2019, to identify the oil just before its arrival on the NE Brazilian coast.

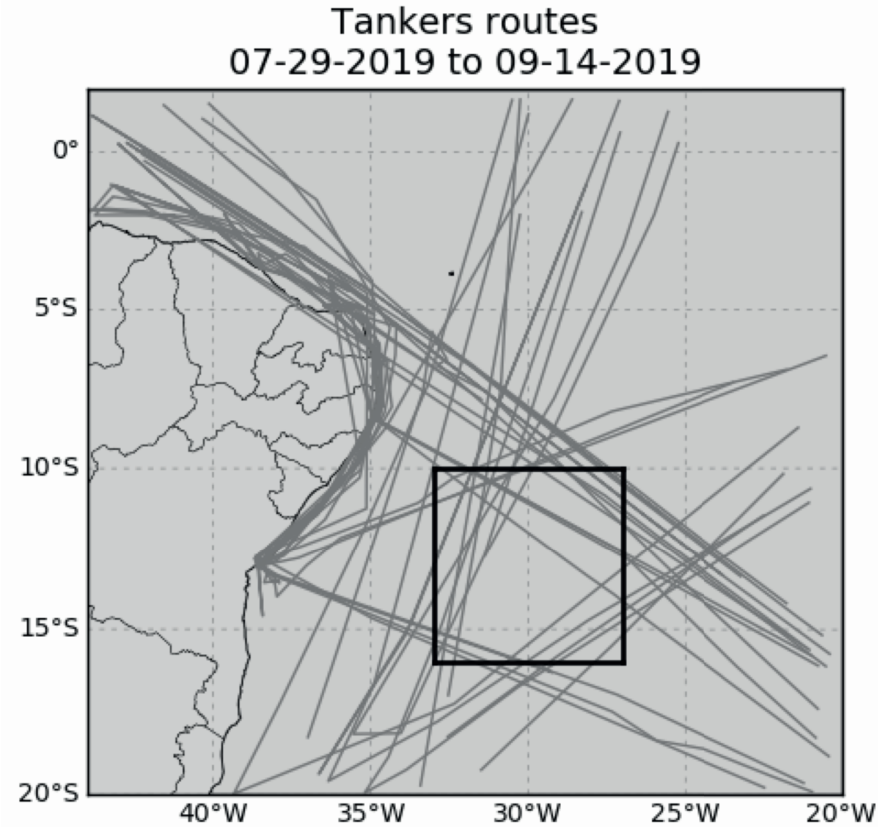

Figure 11. Ship trajectories of oil tankers derived from AIS messages available at CISMAR/MB – Integrated Center for Maritime Security/Brazilian Navy, for the period July 29 to September 14, 2019.

RESULTS AND DISCUSSION

During the last quarter of 2019, Brazil experienced its worst environmental disaster by oil contamination of its beaches in its history. The oil, having reached the shores completely unnoticed, left both society and government agencies completely clueless of its origin, how much oil remained in the ocean still to reach the shorelines and, ultimately, which beaches were going to be affected next. To help answer such questions, which were formulated in real-time during the event, this study utilized the most advanced techniques and data available to scrutinize a number of possibilities for the origin and path of the oil that reached the Brazilian shores. The forensic analyses of the oil samples indicated that the spilled oil density was slightly lower than that of seawater, explaining the problems faced by the response teams in detecting the oil while it was at sea as it traveled below the sea surface.

The backward Lagrangian trajectory simulations for particles at depths of 0 and 15 m corroborate the numerical model simulations using (i) independent models and (ii) satellite-derived velocity fields. These simulations show that the most probable paths of the oil followed the southern branch of the South Equatorial Current, taking initially a fast, more direct path before lingering in a slow, eddy-rich flow, both fitting the probable spill region indicated in Figure 12. Lagrangian trajectories depend on the resolution and accuracy of the velocity fields, and both are bound to improve in the next generation of swath-altimeters (Fu & Ubellmann 2014).

The forward oil spill simulations show that there is a good probability that the oil spill occurred from a mobile source between the

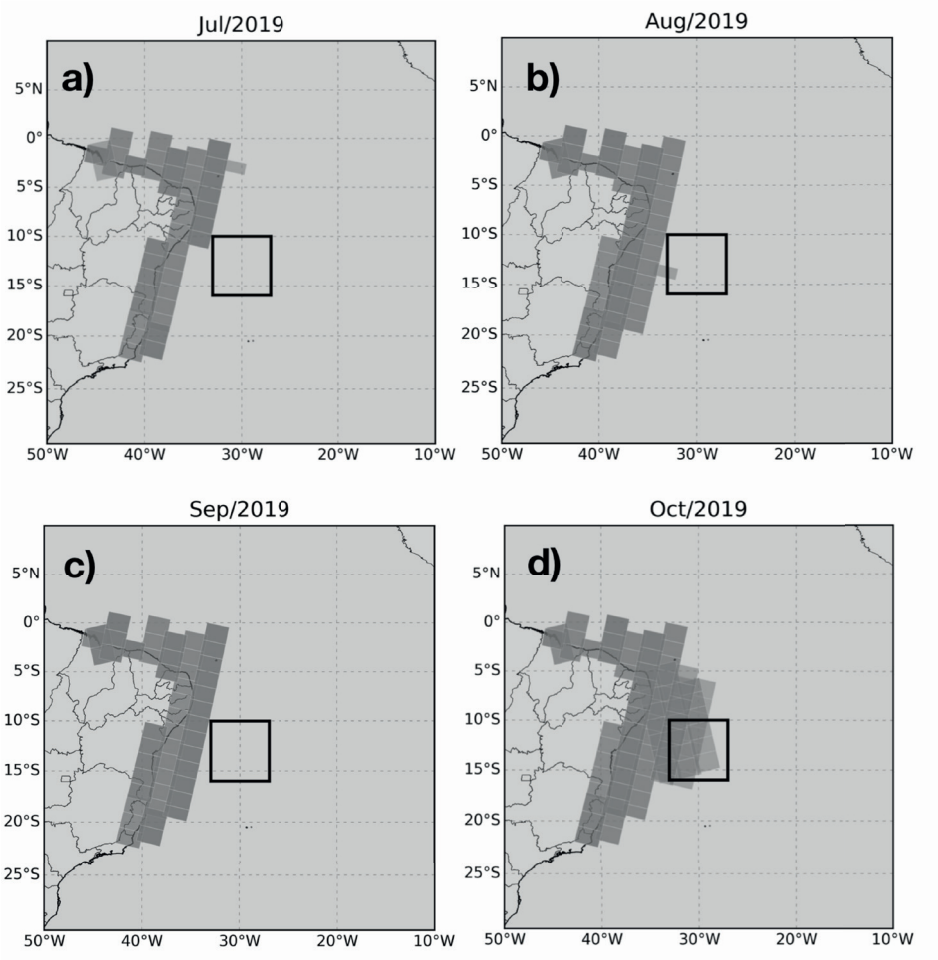

Figure 12. Geographic and monthly distribution of Sentinel-1 scenes available for (a) July, (b) August, (c) September and (d) October, 2019, in the region of study. The black rectangle indicates the region of highest probability of oil spill origin.

latitudes of 10°S and 15°S and the longitudes of 32°W and 28°W, not excluding possible oil tanker routes close to this area. According to the weathering of the oil and its distribution along the Brazilian coast throughout the experiments, and assuming the hypothesis of a superficial spill proportional to the volume of an oil tanker, this simulation study suggested a higher probability that the oil came from one or more sources west of 25°W.

The analysis presented here reveals that the available SAR data set was inadequate for oil spill and ship detection. First, the aerial coverage during July and August, preceding the first oil arrivals, was predominantly in the more coastal region. When a more adequate coverage of the offshore zone was obtained, it was perhaps collected too long after the relevant events to yield any useful results. Because the satellite SAR data was not useful for detecting oil on the surface far offshore or the presence of a nearby ship, the available AIS data was not effective for uncovering a potentially responsible agent. Finally, it should be highlighted that the oil drift modeling, which was performed using the type of heavy oil found on shore, indicated that for such a surface spill, only a fraction of the oil (approximately 40%) would remain on the surface over a maximum period of approximately 10 to 12 days after the spill. With the passing of additional days, a continuous amount of surface oil would have sunk to subsurface layers of the ocean. Therefore, after a period of approximately two weeks from the oil release

at the surface, it would be increasingly more difficult, if not impossible, to detect it using SAR images. Only oil spills on the ocean surface can be detected in SAR images. Hence, only more complete aerial coverage and a more frequent satellite SAR acquisition scheme could have allowed positive detection of the spill and the responsible vessel. These results highlight the need for a continuously operating satellite SAR monitoring program with ample aerial coverage of the "Blue Amazon", the full ocean region bordering Brazilian shores. A Brazilian C or X band SAR satellite mission, focused on ocean monitoring, is therefore highly recommended as part of the Brazilian Space Program.

Future work must include an analysis of the observed in-situ and satellite data, as well as other sources of reanalysis. An analysis of the density fields must also be included as well as an attempt to verify the effects of the environment on the behavior of the oil using oceanographic data with higher time frequencies and spatial resolutions.

Despite the difficult logistical preparation and execution, one or more controlled oil spill simulations in a chosen region of Brazilian waters (as has been done several times in the North Sea) should be considered. This type of experiment should include the release of small, but still significant, amounts of different oil types in separate patches. A pre-scheduled satellite data acquisition scheme (SAR and optical imagery) would guarantee the acquisition of a proper data set of satellite images to allow oil spill and ship detection processing and analysis. The simultaneous release of a number of satellite-tracked surface drifters should provide excellent data for verifying the spreading and drifting behavior of the ocean particles at the experimental site as well as for the calibration and validation of various numerical ocean and oil spill models. Given the higher probability of a medium to large accidental oil spill in a zone of oil exploration or production, the design and implementation of an oil spill experiment in the Campos or Santos Basins, the two main Brazilian oil production sites, might be most interesting.

Acknowledgments

The authors acknowledge the support of the Instituto Nacional de Pesquisas Espaciais - INPE and the Brazilian Navy - MB for their support in the completion of this study. This work was partially supported by Conselho Nacional de Desenvolvimento Científico e Tecnológico - CNPq Grant No. 440857/2020-1, CNPq/MCTI 06/2020 - Pesquisa e Desenvolvimento para Enfrentamento de Derramamento de Óleo na Costa Brasileira, Programa Ciência no Mar, and Coordenação de Aperfeiçoamento de Pessoal de Nível Superior- CAPES finance code 001, the National Institute of Science and Technology for Climate Change Phase 2 under CNPq Grant 465501/2014-1, FAPESP Grant 2014/50848-9 and CAPES Grant 16/2014. The ocean currents and satellite data provided by Copernicus Marine Environment Monitoring Service - CMEMS are acknowledged. Special thanks are dedicated, in memoriam, to Dr. Wiliam Marques, taken from us by COVID-19. Dr. Marques was a vibrant researcher that collaborated extensively from the first moments of the 2019 oil spill, contributing his competence in modeling oil dispersion with tireless enthusiasm and determination.

REFERENCES

AMERICAN PETROLEUM INSTITUTE. 2016. Sunken Oil Detection and Recovery Operational Guide. API Technical Report 1154-1, 1st ed, 126 p.

BARRETO FTC. 2019. Modelling the fate and transport of oil spills. Doctoral thesis in Environmental Engineering. Universidade Federal do Espírito Santo, Espírito Santo, 145 p.

BOURLÈS B ET AL. 2008. The PIRATA Program: History, Accomplishments, and Future Directions. BAMS 89(8): 1111-1126. https://doi.org/10.1175/2008BAMS2462.1.

BOURLÉS B ET AL. 2019. PIRATA: A Sustained Observing System for Tropical Atlantic Climate Research and Forecasting. AGU 6(4): 577-616. https://doi.org/10.1029/2018EA000428.

CIRANO M, MATA MM, CAMPOS EJD & DEIRO NFR. 2006. A Circulação Oceânica de Larga-Escala na Região Oeste do

Atlântico Sul com Base no Modelo de Circulação Global OCCAM. Rev Bras de Geof 24(2): 209-230. https://doi.org/10.1590/S0102-261X2006000200005.

DELANDMETER P & VAN SEBILLE E. 2019. The Parcels v2.0 Lagrangian framework: new field interpolation schemes. GMD 12: 3571-3584. https://doi.org/10.5194/gmd-12-3571-2019.

DREVILLON M ET AL. 2018. Learning about Copernicus Marine Environment Monitoring Service "CMEMS": A Practical Introduction to the Use of the European Operational Oceanography Service. In: Chassignet E, Pascual A, Tintoré J & Verron J (Eds), New frontiers in operational oceanography, GODAE OceanView, p. 695-712. doi:10.17125/gov2018.ch25.

FINGAS M & BROWN CE. 2017. A Review of Oil Spill Remote Sensing. Sensors 18(1): 91. https://doi.org/10.3390/s18010091.

FU L & UBELLMANN C. 2014. On the Transition from Profile Altimeter to Swath Altimeter for Observing Global Ocean Surface Topography. J Atmos Oceanic Technol 31(2): 560-568. https://doi.org/10.1175/JTECH-D-13-00109.1.

HASSELMANN K ET AL. 1973. Measurements of wind-wave growth and swell decay during the Joint North Sea Wave Project (JONSWAP). Ergänzungsheft zur Deutchen HydrographZeitschrift.ReiheA(8°)12:95p.http://resolver.tudelft.nl/uuid:f204e188-13b9-49d8-a6dc-4fb7c20562fc.

IBAMA. 2019. Manchas de óleo no Nordeste. IBAMA. www.ibama.gov.br/manchasdeoleo.

LANGE M & VAN SEBILLE E. 2017. Parcels v0.9: prototyping a Lagrangian ocean analysis framework for the petascale age. Geosci Model Dev 10: 4175-4186. https://doi.org/10.5194/gmd-10-4175-2017.

LEIFER IL ET AL. 2012. State of the art satellite and airborne marine oil spill remote sensing: Application to the BP Deepwater Horizon oil spill. Remote Sens Environ 124: 185-209. https://doi.org/10.1016/j.rse.2012.03.024.

LELLOUCHE JM ET AL. 2018. Recent updates to the Copernicus Marine Service global ocean monitoring and forecasting real-time 1⁄12° high-resolution system. Ocean Sci 14: 1093-1126. https://doi.org/10.5194/os-14-1093-2018.

LOBÃO MM, CARDOSO JN, MELLO MR, BROOKS PW, LOPES CC & LOPES RSC. 2010. Identification of source of a marine oil-spill using geochemical and chemometric techniques. Mar Pollut Bull 60(12): 2263-2274. https://doi.org/10.1016/j.marpolbul.2010.08.008.

LÓPEZ J & MÓNACO SLO. 2017. Vanadium, nickel and sulfur in crude oils and source rocks and their relationship with biomarkers: Implications for the origin of crude oils in Venezuelan basins. Org Geochem 104: 53-68. https://doi.org/10.1016/j.orggeochem.2016.11.007.

MIRANDA FP, FONSECA LEN, BEISL CH, ROSENQVIST A & FIGUEIREDO MDMAM. 1997. Seasonal mapping of flooding extent in the vicinity of the Balbina Dam (Central Amazonia) using RADARSAT-1 and JERS-1 SAR data. In: International Symposium, INPE, 5981 p.

MIRANDA FP, MARMOL AMQ, PEDROSO EC, BEISL CH, WELGAN P & MORALES LM. 2004. Analysis of RADARSAT-1 data for offshore monitoring activities in the Cantarell Complex, Gulf of Mexico, using the unsupervised semivariogram textural classifier (USTC). Can J Remote Sens 30(3): 424-436. https://doi.org/10.5589/m04-019.

NOAA 2019. 2019 Marine Pollution Surveillance Reports, Office of Satellite and Product Operations. https://www.ospo.noaa.gov/Products/ocean/marinepollution/2019_archive.html.

NORTHERN GATEWAY PIPELINES INC. 2010. Section 3.9: Ship Specifications TERMPOL Surveys and Studies. In: Enbridge Northern Gateway Project Final – REV 0: 37 p.

OLIVEIRA OMC, QUEIROZ AFS, CERQUEIRA JR, SOARES SAR, GARCIA KS, PAVANI FILHO A, ROSA MLS, SUZART CM, PINHEIRO LL & MOREIRA ITA. 2020. Environmental disaster in the northeast coast of Brazil: Forensic geochemistry in the identification of the source of the oily material. Mar Pollut Bull 160(111597): 1-7. https://doi.org/10.1016/j.marpolbul.2020.111597.

PETERS KE, WALTERS CC & MOLDOWAN JM. 2005. The Biomarker Guide Volume 1 - Biomarkers and Isotopes in the Environment and Human History, 2nd ed, UK: Cambridge University Press, p. 1-2.

PRASAD SJ, FRANCIS PA, BALAKRISHNAN NAIR TM, SHENOI SSC & VIJAYALAKSHMI T. 2019. Oil spill trajectory prediction with high-resolution ocean currents. J Oper Oceanogr 13(2): 84-99. https://doi.org/10.1080/1755876X.2019.1606691.

REED M, JOHANSEN O, BRANDVIK PJ, DALING P, LEWIS A, FIOCCO R, MACKAY D & PRENTKI R. 1999. Oil spill modeling towards the close of the 20th century: Overview of the state of the art. Spill Sci Technol Bull 5(1): 3-16.https://doi.org/10.1016/S1353-2561(98)00029-2.

RIO MH, MULET S & PICOT N. 2014. Beyond GOCE for the ocean circulation estimate: Synergetic use of altimetry, gravimetry, and in situ data provides new insight into geostrophic and Ekman currents. Geophys Res Lett 41(24): 8918-8925. https://doi.org/10.1002/2014GL061773.

RODRIGUES RR, ROTHSTEIN LM & WIMBUSH M. 2007. Seasonal variability of the South Equatorial Current bifurcation

in the Atlantic Ocean: A numerical study. J Geophys Res 37(1): 16-30. https://doi.org/10.1175/jpo2983.1.

SILVA M, ARAUJO M, SERVAIN J, PEVEN P & LENTINI CAD. 2009. High resolution regional ocean dynamics simulation in the southwestern tropical Atlantic. Ocean Model 30(4): 256-269. https://doi.org/10.1016/j.ocemod.2009.07.002.

SILVEIRA ICA, CALADO L, CASTRO BM, CIRANO M, LIMA JAM & MASCARENHAS ADS. 2004. On the baroclinic structure of the Brazil Current-intermediate Western boundary current system. Geophys Res Lett 31(14): L14308. https://doi.org/10.1029/2004GL020036.

SILVEIRA ICA, SCHMIDT ACK, CAMPOS EJD, GODOI SS & IKEDA Y. 2000. A Corrente do Brasil ao largo da costa leste brasileira. R Bras Oceanogr 48(2): 171-183.

SISSINI MN ET AL. 2020. Brazil oil spill response: Protect rhodolith beds. Science 367(6474): 156. https://doi.org/10.1126/science.aba2582.

SOUTELINO RG, GANGOPADHYAY A & SILVEIRA ICA. 2013. The roles of vertical shear and topography on the eddy formation near the site of origin of the Brazil Current. Cont Shelf Res 70: 46-60. https://doi.org/10.1016/j.csr.2013.10.001.

SOUTELINO RG, SILVEIRA ICA, GANGOPADHYAY A & MIRANDA JA. 2011. Is the Brazil Current eddy-dominated to the north of 20oS?. Geophys Res Lett 38(3): L03607. https://doi.org/10.1029/2010GL046276.

STOUT SA & WANG Z. 2007. Chemical fingerprinting of spilled or discharged petroleum-methods and factors affecting petroleum fingerprints in the environment. In: Wang Z & Stout SA (Eds). Oil Spill Environ Forensics 1: 1-53.

TESSAROLO LF. 2017. Numerical model for oil and gas releases from deepwater: Validation and applications in hypothetical blowouts. Doctoral Thesis in Meteorology. Instituto Nacional de Pesquisas Espaciais, 256 p.

WANG Z, STOUT SA & FINGAS M. 2006. Forensic Fingerprinting of Biomarkers for Oil Spill Characterization and Source Identification. Environ Forensics 7(2): 105-146. https://doi.org/10.1080/15275920600667104.

How to cite

NOBRE P ET AL. 2022. The 2019 northeast Brazil oil spill: scenarios. An Acad Bras Cienc 94: e20210391. DOI 10.1590/0001-3765202220210391.

Manuscript received on March 18, 2021;
accepted for publication on August 09, 2021

PAULO NOBRE[1]
https://orcid.org/0000-0001-9061-4556

ANGELO T. LEMOS[2]
https://orcid.org/0000-0003-1229-9807

EMANUEL GIAROLLA[1]
https://orcid.org/0000-0003-0810-574X

ROSIO CAMAYO[1]
https://orcid.org/0000-0002-2362-5631

LAERCIO NAMIKAWA[1]
https://orcid.org/0000-0001-7847-1804

MILTON KAMPEL[1]
https://orcid.org/0000-0002-0011-2083

NATÁLIA RUDORFF[1]
https://orcid.org/0000-0003-3451-4512

DIEGO X. BEZERRA[1]
https://orcid.org/0000-0003-2599-696X

JOÃO LORENZZETTI[1]
https://orcid.org/0000-0003-3752-1021

JORGE GOMES[1]
https://orcid.org/0000-0003-2235-171X

MANOEL B. DA SILVA JR[1]
https://orcid.org/0000-0003-0101-9013

CARLA P.M. LAGE[3]
https://orcid.org/0000-0002-5019-9308

RAFAEL L. PAES[4]
https://orcid.org/0000-0003-3599-8512

CARLOS BEISL[5]
https://orcid.org/0000-0002-0106-0633

MÁRCIO M. LOBÃO[6]
https://orcid.org/0000-0002-8388-0490

PEDRO A. BIGNELLI[7]
https://orcid.org/0000-0001-5573-7665

NAJLA DE MOURA[7]
https://orcid.org/0000-0002-8536-0640

WOUGRAN S. GALVÃO[7]
https://orcid.org/0000-0002-7467-4679

PAULO S. POLITO[8]
https://orcid.org/0000-0003-2217-3853

[1]Instituto Nacional de Pesquisas Espaciais (INPE), Av. dos Astronautas, 1758, Jardim da Granja, 12227-010 São José dos Campos, SP, Brazil

[2]Universidade Federal do Sul da Bahia (UFSB), Rodovia de Acesso para Itabuna, Km 39, 45613-204 Porto Seguro, BA, Brazil

[3]Diretoria de Gestão de Programas da Marinha (DgePM), Rua 1° de Março, 118, Ed. Barão de Ladário, 10° Andar, Centro, 20010-000 Rio de Janeiro, RJ, Brazil

[4]Instituto de Estudos Avançados (IEAv), Trevo Coronel Aviador José Alberto Albano do Amarante, 1, Putim, 12228-001 São José dos Campos, SP, Brazil

[5]Universidade Federal do Rio de Janeiro (UFRJ), Av. Pedro Calmon, 550, Cidade Universitária, 21941-901 Rio de Janeiro, RJ, Brazil

[6]Instituto de Estudos do Mar Almirante Paulo Moreira (IEAPM), Rua Kioto, 253, Praia dos Anjos, 28930-000 Arraial do Cabo, RJ, Brazil

[7]Instituto Brasileiro do Meio Ambiente e dos Recursos Naturais Renováveis (IBAMA), SCEN Trecho 2, Edifício Sede, L4 Norte, 70818-900 Brasília, DF, Brazil

[8]Universidade de São Paulo (USP), Rua da Praça do Relógio, 109, Butantã, 05508-050 São Paulo, SP, Brazil

Correspondence to: **Paulo Nobre**
E-mail: paulo.nobre@inpe.br

Author contributions

Paulo Nobre: Coordinated the contributions; Angelo T. Lemos: Computed oil dispersion simulations; Emanuel Giarolla: Computed back trajectories; Rosio Camayo: Computed ocean states; Laercio Namikawa, Milton Kampel, Natália Rudorff and Carlos Beisl: Contributed with satellite analyses., Diego X. Bezerra, João Lorenzzetti , Carla P. M. Lage and Rafael L. Paes: Contributed with ship tracking analyzes; Jorge Gomes: Contributed with atmospheric modeling; Manoel B. da Silva Jr.: Contributed with the numerics of atmos, ocean modeling; Márcio M. Lobão: Contributed with oil chemical analyses; Pedro A. Bignelli, Najla de Moura and Wougran Soares Galvão: Contributed with oil spill data; Paulo S. Polito: Contributed with back trajectory calculations.